Electrostatic Effects in Highly Charged Proteins: Salt Sensitivity of pK_a Values of Histidines in Staphylococcal Nuclease†

Kelly K. Lee,‡ Carolyn A. Fitch,‡ Juliette T. J. Lecomte,§ and Bertrand García-Moreno E.*,‡

Department of Biophysics, Johns Hopkins University, 3400 North Charles Street, Baltimore, Maryland 21218, and Chemistry Department, The Pennsylvania State University, University Park, Pennsylvania 16802

Received October 17, 2001

ABSTRACT: The pK_a values of most histidines in small peptides and in myoglobin increase on average by 0.30 unit between 0.02 and 1.5 M NaCl [Kao et al. (2000) *Biophys. J. 79*, 1637]. The ΔpK_a values reflect primarily the ionic strength dependence of the solvation energy; screening of Coulombic interactions contributes only in a minor way. This implies that Coulombic interactions are weak, or that attractive and repulsive contributions to the pK_a values are balanced. To distinguish experimentally between these two possibilities, and to further characterize the magnitude and salt sensitivity of surface electrostatic interactions in proteins, the salt dependence of pK_a values of histidines in staphylococcal nuclease was measured by ^{1}H NMR spectroscopy. Three of the four histidines titrated with significantly depressed pK_a values, and the salt sensitivity of all histidine pK_a values was substantial. In three cases, the pK_a values increased by a full unit between 0.01 and 1.5 M KCl. Anion-specific effects were found; the pK_a values measured under equivalent ionic strengths in SCN^- and SO_4^{2-} were higher than in Cl^-; the order of the sensitivity of pK_a values to anions was $SCN^- > Cl^- > SO_4^{2-}$. Structure-based pK_a calculations with continuum methods were performed to interpret the measured effects structurally and to test their ability to capture the experimental behavior. Calculations in which the protein interior was treated empirically with a dielectric constant of 20 reproduced the pK_a values and their dependence on the concentration of Cl^-. According to the calculations, the pK_a values are depressed because of unfavorable self-energies and repulsive Coulombic interactions. Their striking salt sensitivity reflects screening of weak, repulsive, Coulombic interactions among charges separated by more than 10 Å. Long-range Coulombic interactions on the surfaces of proteins are weak, but they can add up to produce substantial electrostatic effects when positive and negative charges are not balanced.

Electrostatic interactions contribute significantly to the structure, function, and stability of many proteins and macromolecular assemblies. Our understanding of the physical character and structural origins of electrostatic effects in proteins has been advanced considerably through structure-based calculations of electrostatic energy and pK_a values. However, recent experimental studies have challenged some of the notions borne mainly from calculations, thus renewing interest in further experimental characterization of electrostatic effects in proteins. For example, in conflict with one of the underlying assumptions in calculations of electrostatic contributions to stability, it has been shown with several proteins that significant electrostatic interactions can be present in denatured states (*1*−*6*). It has also been demonstrated that ionizable residues can be buried in the hydrophobic interior of proteins, which contradicts expectations based on the treatment of the protein interior as a medium of low polarizability in continuum models (*7*−*10*). In general, electrostatic effects measured experimentally are weaker than those estimated with structure-based methods (*11*−*15*). Weak electrostatic interactions among surface residues are consistent with the observation that the pH of maximum stability is not correlated with the isoionic point of a protein (*16*). However, they are not so weak as to exclude the possibility of enhancing the stability of proteins by rational modification of surface ionizable residues, as demonstrated recently in several proteins (*16*−*19*). Further experimental studies to improve our understanding of the magnitude of surface electrostatic interactions, their dependence on environmental factors such as temperature and ionic strength, and their contributions to the stability of proteins are clearly warranted. Here we present an experimental study of the salt sensitivity of histidine pK_a values in a highly charged protein.

In a previous study, the salt sensitivity of pK_a values of histidines in myoglobin from sperm whale and horse heart was found to be modest and indistinguishable from that of histidines in peptides (*12*). On average, the pK_a values of most histidines increase by 0.30 unit between 0.02 and 1.5 M NaCl, regardless of the character of their local environments. The notable exceptions are a histidine whose elevated pK_a is insensitive to salt, and a histidine whose depressed pK_a is steeply dependent on salt concentration; the first is ion-paired to a glutamate, and the second is in van der Waals

† This work was supported by NSF Grant MCB-9600991 to B.G.-M.E.

* Correspondence should be addressed to this author. Tel: (410) 516-4497. FAX: (410) 516-4118. Email: bertrand@jhu.edu.

‡ Johns Hopkins University.

§ The Pennsylvania State University.

10.1021/bi0119417 CCC: $22.00
Published on Web 04/06/2002

contact with an arginine. The pK_a of the histidine in the peptide Phe-Lys-His-Leu-Lys (FKHLK) is also depressed and strongly salt dependent, presumably because the repulsive interactions with the net +2 charge of the peptide are screened effectively by counterions.

The similarities in the measured salt dependence of pK_a values of most histidines in myoglobin and in neutral peptides suggest that the influence by the environment of the histidines in the protein is modest. The salt effect was thus interpreted in terms of a shift in the equilibrium between neutral and charged forms of histidine in favor of the charged species at high salt concentration, driven by attractive electrostatic interactions between histidinium and counteranions. This interpretation was supported by continuum electrostatics calculations of the ionic strength dependence of the solvation energy of imidazole, calculated from differences in the self-energy of the charged and neutral species in a vacuum and in solution. According to the calculations, solvation energies can account for an increase of 0.20 unit in the pK_a of imidazole between ionic strengths of 0.02 and 1.5 M (*12*).

The conclusion that screening of Coulombic interactions among surface charges is not the dominant factor that determines the salt sensitivity of histidine pK_a values in myoglobin contradicts the results of continuum calculations (*12*). The absence of Coulombic contributions to the histidine pK_a values can be explained in two ways. Either pairwise electrostatic interactions are weak, or attractive and repulsive contributions are balanced, in which case increasing ionic strength could screen these interactions substantially without having a measurable effect on the pK_a values.

Linderstrøm-Lang first suggested that in proteins the salt dependence of pK_a values is determined by their distance to the isoionic point (*20*). At the isoionic point, the net charge of a protein is zero. At pH values below their isoionic point, proteins are positively charged; at pH values above it, they bear net negative charge. In proteins with relatively symmetrical charge distributions, attractive and repulsive, medium- and long-range electrostatic interactions are balanced at the isoionic point. Under these conditions, every attractive interaction is canceled by a repulsive interaction, and globally the protein becomes insensitive to changes in salt concentration. At extreme pH values, or in proteins with asymmetric charge distributions, charge imbalance exists, which can lead to significant salt sensitivity, especially if medium- and long-range interactions are strong.

Histidine pK_a values were measured in staphylococcal nuclease (SNase) by ^{1}H NMR spectroscopy to assess quantitatively the magnitude and salt-dependence of Coulombic interactions among surface ionizable residues, and their contributions to pK_a values. SNase was selected because it is highly charged; it has 32 basic and 20 acidic residues, yielding an isoionic point greater than 10.2 (Fitch, Whitten, and García-Moreno, unpublished experiments), higher than the isoionic point of 8.2 of sperm whale myoglobin (*21*). The net positive charge likely represents a functional adaptation to enhance the ability of this nuclease to recognize nucleic acids nonspecifically through electrostatic interactions. The practical implication of the high net charge of SNase for these studies is that it allowed measurement of proton binding equilibria under conditions where the protein has a substantial net positive charge. pK_a values were measured in the absence of added salt and in 0.02, 0.10, 0.50, and 1.5 M KCl. The effects of chloride (Cl^-), sulfate (SO_4^{2-}), and thiocyanate (SCN^-) ions were compared in an attempt to dissect the salt effect into specific and nonspecific contributions. Structure-based pK_a calculations were performed with semi-macroscopic continuum methods to interpret the structural origins of the measured energetics and to test the ability of the computational methods to reproduce the salt dependence of pK_a values quantitatively. This study contributes physical insight about the unusual salt dependence of electrostatic effects in highly charged proteins. The pK_a values that are presented also constitute benchmarks necessary to test computational methods for structure-based calculations of electrostatic energy.

MATERIALS AND METHODS

Protein and Peptide Samples. SNase was expressed and purified following the procedure described previously by Shortle and Meeker (*22*). The protein was established to be >95% pure by SDS−PAGE. Protein concentration was determined at 280 nm using an optical density of 0.93 (*23*).

Measurement of pK_a Values by ^{1}H NMR Spectroscopy. Procedures for the acid/base titration of histidines in SNase and peptides monitored by NMR spectroscopy are those reported elsewhere (Fitch, Lee, Karp, Stites, Lattman, and García-Moreno, *Biophys. J.*, in press) (*12*, *24*−*26*). Samples were prepared by exchange of H_2O for D_2O to approximately 99% completion by successive dilution in Centricon-10 tubes (Millipore Corp.), and by heating the samples to 45 °C (approximately 10 °C below the temperature midpoint for SNase denaturation) for 15 min. The salt concentration was adjusted with stock solutions of 3 M KCl, 0.4 M K_2SO_4, or 3 M KSCN in D_2O (Isotec, Inc.). Final protein concentrations typically were in the range 0.6−1.0 mM. Within the range of protein concentrations 0.6−1.2 mM, the pK_a values of histidines in SNase were identical.

Histidine-containing peptides cyclo-Gly-His (cGH) and pyro-Glu-His-Gly-NH_2 (pEHGa) were obtained in powder form (Bachem, Sigma, respectively) and used without further purification. The pentapeptide Phe-Lys-His-Leu-Lys (FKHLK) was synthesized at the Johns Hopkins Protein Synthesis Facility by Fmoc chemistry and purified by reverse-phase HPLC. Its composition was verified by mass spectrometry. The peptides were dissolved in D_2O, and the salt concentration was adjusted with stock salt solutions. The concentration of cGH, pEHGa, and FKHLK used was 15, 3, and 5 mM, respectively. Based on repeated titrations of some of these peptides, it was established that the measured pK_a values were not influenced by peptide concentration.

^{1}H NMR spectra were recorded on a 500 MHz Varian Unity Plus spectrometer using standard parameters for a diamagnetic protein (Fitch, Lee, Karp, Stites, Lattman, and García-Moreno, *Biophys. J.*, in press). All spectra were referenced against the position of the HDO peak. The mean value of the HDO chemical shift was determined by averaging the HDO chemical shift, referenced to the 1 mM DSS (2,2-dimethyl-2-silapentane-5-sulfonate, Sigma) internal standard that was used at both the acidic and the basic extrema of each titration. The chemical shift of the primary DSS peak is insensitive to changes in pH and ionic strength (*27*). Changes in the chemical shift of HDO referenced in the manner described never exceeded 0.013 ppm over the

course of a titration. This is consistent with the expected pH dependence of the HDO resonance, and considerably less than the 1 ppm shift observed over the course of the titration for the resonance of Cϵ1H used to monitor the ionization state of the histidines. Spectra collected in the presence and absence of DSS under otherwise identical conditions were indistinguishable. The reported pH values are pH readings measured immediately following data acquisition; they were not corrected for deuterium isotope effects (*28*, *29*). pH was read with a PHM-95 pH/ion meter (Radiometer) and a combination electrode (Wilmad Glass) calibrated with standard solutions (Fisher Scientific) at pH 4.00 and 10.00 at 25 °C. Spectra were recorded at 25 °C. The temperature of samples in the NMR probe was calibrated using a MeOH standard solution (Wilmad Glass). DCl (Isotec) and KOD (Aldrich) were used to adjust the pH of the samples.

Acid/base titrations were performed with no added salt and in 0.02, 0.10, 0.50, and 1.5 M KCl. In the case where no salt was added, an average ionic strength of 0.01 M was assumed, based on the amounts of acid or base used in the titration. Salt concentrations of 0.0067, 0.033, and 0.167 M for experiments in K_2SO_4 were used to reproduce the ionic strengths of 0.02, 0.10, and 0.50 M used with monovalent salts.

Data were processed as described elsewhere (Fitch, Lee, Karp, Stites, Lattman, and García-Moreno, *Biophys. J.*, in press). The state of protonation of each histidine was assessed with the chemical shift of the Cϵ1H resonance. The position of this signal is known to be independent of protein concentration; thus, it reports on the monomeric state (*30*). Minor signals arising from isomerization of the Lys-116−Pro-117 bond were ignored. The pK_a values of histidines were obtained by fitting plots of the chemical shift of the Cϵ1H resonance versus pH with a modified Henderson−Hasselbalch equation applicable to fast exchange situations (*31*):

$$\delta(\mathrm{pH}) = \delta_+ - (\delta_+ - \delta_o)\frac{10^{n(\mathrm{pH}-\mathrm{p}K_a)}}{1 + 10^{n(\mathrm{pH}-\mathrm{p}K_a)}} \qquad (1)$$

In this equation, δ_o is the chemical shift of the neutral imidazole, δ_+ is the chemical shift of the imidazolium ion, δ(pH) is the chemical shift at a given pH value, n is a phenomenological Hill coefficient, and pK_a is the apparent ionization constant. n, pK_a, δ_+, and δ_o were floated in the fitting procedure. The values of n did not vary more than ±20% in the different ionic conditions studied. The pK_a values that were resolved when n was fixed at 1 were identical to the values resolved when n was floated.

Structure-Based pK_a Calculations. pK_a calculations were performed with the finite-difference Poisson−Boltzmann method described previously (*13*, *14*). Electrostatic potentials were calculated with the University of Houston Brownian Dynamics package (*32*). Charge states were determined with the statistical thermodynamic method of Gilson (*33*). The implementation used here follows the procedure described for staphylococcal nuclease (Fitch, Lee, Karp, Stites, Lattman, and García-Moreno, *Biophys. J.*, in press). The adjustable parameters were $\epsilon_{in} = 20$, $\epsilon_{water} = 78.5$, $T = 298$ K, Stern layer = 2.0 Å, and probe radius = 1.4 Å. All calculations were performed with the Protein DataBank structure 1stn. The first five and the last eight residues of this structure are invisible (*34*). This includes 5 charge groups: Lys-5, Glu-142, Asp-143, Asp-146, and the carboxyl terminus. These charges were not included in the calculation, tantamount to assuming that they are very well screened and not sensed electrostatically by the rest of the protein.

The linearized form of the Poisson−Boltzmann equation is not formally valid at the high ionic strengths that were studied experimentally. However, the empirical observation has been made previously that the calculated pK_a values and electrostatic energies are reasonable even in ionic strengths as high as 1.5 M (*12*). The present calculations were repeated with the nonlinearized form of the Poisson−Boltzmann equation, and the results were indistinguishable from those obtained with the linearized equation (data not shown).

RESULTS

Effects of KCl on pK_a Values. Acid/base titrations of SNase were performed by ^{1}H NMR spectroscopy in 0.02, 0.10, 0.50, and 1.5 M KCl. Samples dialyzed extensively in water in the absence of added salt were also studied; at extreme pH values, these samples contained approximately 0.01 M Cl^- or K^+. The one-dimensional spectra showed no evidence of any significant salt or pH-induced conformational transition; the dispersion suggested that SNase was in the native state under the conditions of pH and KCl concentration that were studied. This was corroborated by titrations monitored by intrinsic fluorescence; no global conformational changes were observed in acid−base titrations over the range of salt concentrations studied experimentally, nor in salt titrations at pH 5, 7, and 9 from 0 to 2 M KCl (data not shown). Panels A through D in Figure 1 contain chemical shift versus pH plots for His-8 (A), His-46 (B), His-121 (C), and His-124 (D). Increasing KCl concentration shifted the titration curves toward the basic range of pH, as observed previously in myoglobin and in model compounds (*12*). However, the response of histidine residues in SNase was considerably more pronounced than in those other cases.

Complete titrations of His-8, His-46, and His-124 were achieved in the pH range 4−9. In low concentrations of salt, the acid branch of the titration of His-121 was incomplete because of the onset of acid denaturation. However, enough data points were collected to allow robust fitting to obtain pK_a values. In the acid limit, the chemical shifts of His-8 and His-46 were insensitive to salt concentration. The chemical shift of His-124 exhibited some salt dependence, especially in the higher KCl concentration. In the basic limit, the chemical shifts of His-8, His-121, and His-124 were insensitive to salt, whereas His-46 exhibited a mild salt sensitivity.

The pK_a values measured at five different KCl concentrations are listed in Table 1. The reported errors in these values are standard errors of the fit. The magnitude of this error is comparable to the standard deviation of 0.03 determined by three independent measurements of pK_a values in 0.1 M KCl. The measured values are consistent with previously reported values measured in 0.30 M (*30*). At low salt concentrations, three of the four histidines, His-46, His-121, and His-124, have pK_a values that are substantially depressed relative to the pK_a values of histidines in model compounds at comparable ionic strengths. Only His-8 titrated with a pK_a value comparable to that of a histidine in water. The pK_a values of all SNase histidines were clearly sensitive to salt.

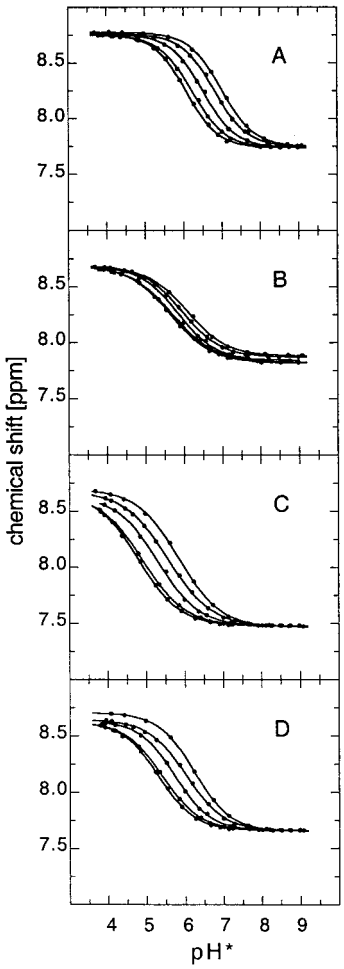

FIGURE 1: Proton binding isotherms monitored by chemical shift position of the Cϵ1H proton of His-8 (A), His-46 (B), His-121 (C), and His-124 (D). Titration curves obtained with no added salt and 0.02, 0.10, 0.50, and 1.50 M KCl are shown (left to right). Filled circles are the measured data points. Solid lines represent fits with eq 1.

Increasing the KCl concentration from 0.01 to 1.5 M increased the pK_a values of His-8, His-46, His-121, and His-124 by 0.92, 0.44, 1.05, and 0.93 pK_a units, respectively, with an error of $\pm$0.06 unit. The data in Figure 2 show that the dependence of pK_a on log [KCl] was approximately linear for all four histidines over the entire range of salt concentration studied. His-121, which titrated with the lowest pK_a value, was also the most sensitive to salt. However, there did not appear to be any further correlation between the response to salt and the deviation from the normal pK_a value as the effects of KCl on the pK_a values of His-8 and of His-124 were also significant. The pK_a of His-46 had the shallowest dependence on KCl concentration although it is still considerably more salt sensitive than most cases studied previously (*12*). At the highest salt concentration, 1.5 M, the pK_a values of three of the four histidines did not reach the normal value of histidine in water, which is between 6.3 and 6.6.

Effects of K_2SO_4 and KSCN on pK_a Values. To explore the molecular origins of the salt dependence of pK_a values, the titrations were also performed in the presence of K_2SO_4 and KSCN. The intention was to dissect the salt effect into nonspecific or indirect contributions by the ionic strength, and specific contributions from more direct, chemical interactions between anions and protein. SCN^- and SO_4^{2-} were selected for these studies because they lie at opposite

Table 1: pK_a Values of Histidines in SNase Measured as a Function of KCl, K_2SO_4, and KSCN Concentration, and Calculated by Continuum Electrostatics Methods[a]

salt concentration	His-8	His-46	His-121	His-124
no added salt[b]	6.08 $\pm$ 0.02	5.66 $\pm$ 0.03	4.80 $\pm$ 0.04	5.31 $\pm$ 0.02
KCl				
0.02 M	6.24 $\pm$ 0.03	5.71 $\pm$ 0.02	4.91 $\pm$ 0.03	5.41 $\pm$ 0.02
0.10 M	6.52 $\pm$ 0.03	5.86 $\pm$ 0.04	5.30 $\pm$ 0.06	5.73 $\pm$ 0.02
0.50 M	6.81 $\pm$ 0.02	5.95 $\pm$ 0.02	5.56 $\pm$ 0.02	6.03 $\pm$ 0.03
1.50 M	7.00 $\pm$ 0.03	6.10 $\pm$ 0.04	5.85 $\pm$ 0.03	6.24 $\pm$ 0.02
K_2SO_4[c]				
0.0067 (0.02 M)	6.41 $\pm$ 0.01	5.77 $\pm$ 0.02	5.20 $\pm$ 0.02	5.62 $\pm$ 0.02
0.033 (0.10 M)	6.66 $\pm$ 0.02	5.89 $\pm$ 0.02	5.47 $\pm$ 0.02	5.89 $\pm$ 0.02
0.167 (0.50 M)	6.88 $\pm$ 0.03	5.98 $\pm$ 0.02	5.66 $\pm$ 0.02	6.09 $\pm$ 0.02
KSCN				
0.10 M	6.62 $\pm$ 0.03	6.01 $\pm$ 0.04	5.53 $\pm$ 0.04	5.98 $\pm$ 0.05
0.50 M	6.97 $\pm$ 0.02	6.30 $\pm$ 0.03	6.12 $\pm$ 0.03	6.45 $\pm$ 0.04
calculated values				
0.01 M	5.96	4.98	4.51	5.43
0.10 M	6.35	5.43	5.18	5.96
0.50 M	6.51	5.66	5.60	6.20
1.50 M	6.55	5.75	5.78	6.27

[a] Error bars reflect goodness of fits to experimental data. [b] Estimated ionic strength when no salt is added is 0.01 M. [c] Values in parentheses refer to the ionic strength.

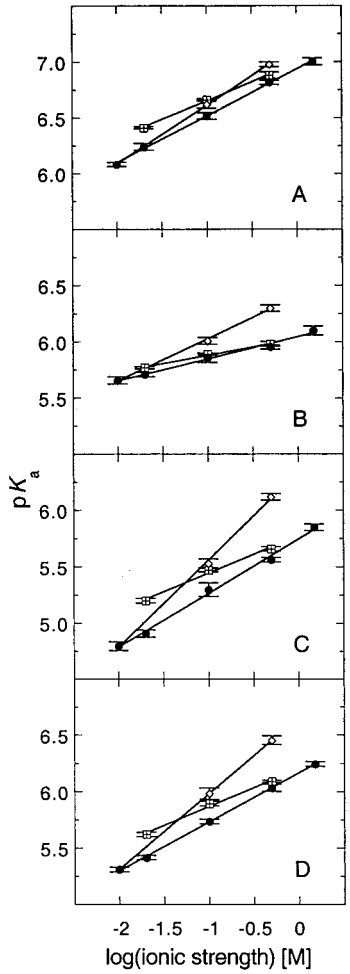

FIGURE 2: Salt dependence of pK_a values measured in KCl (solid circles), K_2SO_4 (hatched squares), and KSCN (open diamonds) for His-8 (A), His-46 (B), His-121 (C), and His-124 (D). Straight lines are only meant to guide the eye.

extremes of the Hofmeister series, which ranks anions according to their inherent potential for direct interactions with proteins (*35*). Cl^- lies in the middle of this series, and its screening effects on electrostatic interactions are more readily interpreted in terms of ionic strength than for other anions.

The effects of KCl, KSCN, and K_2SO_4 were measurably different, as shown by the data in Table 1 and in Figure 2. The pK_a values measured in SCN^- were systematically higher than the values measured in Cl^- under equivalent conditions of ionic strength. The values measured in SO_4^{2-} were also slightly higher than those measured in Cl^-, especially at low salt concentrations. The behavior of the different histidines was not uniform; for example, His-46 was indifferent to the change from Cl^- to SO_4^{2-}. The increase in pK_a values with increasing salt concentration in the presence of SO_4^{2-} was monotonic and not as steep as with Cl^-. Based on the two concentrations of SCN^- that were studied, the dependence of pK_a values appears to be steeper for SCN^- than for Cl^-.

Effects of KSCN on pK_a Values of Histidines in Model Compounds. The pK_a values of histidines in model peptides provide the reference behavior necessary for interpreting the structural and physical determinants of pK_a values in proteins. The NaCl sensitivity of histidine pK_a values in model peptides was described previously (*12*). To understand better how the protein environment contributes to the strong effect of SCN^- on the pK_a values of histidines in SNase, acid/base titrations of histidine-containing compounds were also monitored by ^1H NMR spectroscopy in the presence of KSCN to compare against previous values obtained in NaCl. The pK_a of cGH in 0.50 M NaCl was 6.43 ± 0.02, compared to 6.39 ± 0.06 in 0.50 M KSCN. The pK_a of the histidine in pEHGa in 0.50 M NaCl was 6.47 ± 0.02; in 0.50 M KSCN, it was 6.66 ± 0.02. In FKHLK, the pK_a of the histidine in 0.50 M NaCl was 6.60 ± 0.02; in 0.50 M KSCN, the measured pK_a was 6.80 ± 0.01. KSCN had a small but discernible effect on the pK_a of the histidines in FKHLK and pEHGa, and no effect on the pK_a of the histidine in cGH. The effect on FKHLK is not unexpected because this peptide has a net charge of +2, and SCN^- and SO_4^{2-} interact more strongly with basic groups than Cl^- (*36, 37*). The effect on pEHGa is more difficult to rationalize because, like cGH, it contains no additional charges. Most significantly, the magnitude of the effect of SCN^- on pK_a values of histidines in model compounds is lower than for histidines in SNase, especially His-121 and His-124, which titrate in 0.5 M SCN^- with pK_a values that are on average 0.4 unit higher than in Cl^-.

Structure-Based pK_a Calculations. The pK_a values calculated for the four histidines with continuum methods based on the finite-difference solution of the linearized Poisson−Boltzmann equation are listed in Table 1. It has been recognized previously that the strength of electrostatic interactions among surface residues is exaggerated in this type of calculation when a single protein conformation is used and when the protein interior is treated with a dielectric constant (ϵ_{in}) of 4 (*12, 13, 38*). It is thought that this low value of ϵ_{in} underestimates the consequences of structural reorganization upon ionization of charged sites on pK_a values (*13, 39*). To maximize the agreement between calculated and measured pK_a values in these calculations, the protein interior was treated with the empirical value of $\epsilon_{in} = 20$ (*13*). With $\epsilon_{in} = 20$, the agreement between the experimental and the calculated pK_a values, especially in 0.10 M KCl, was very good.

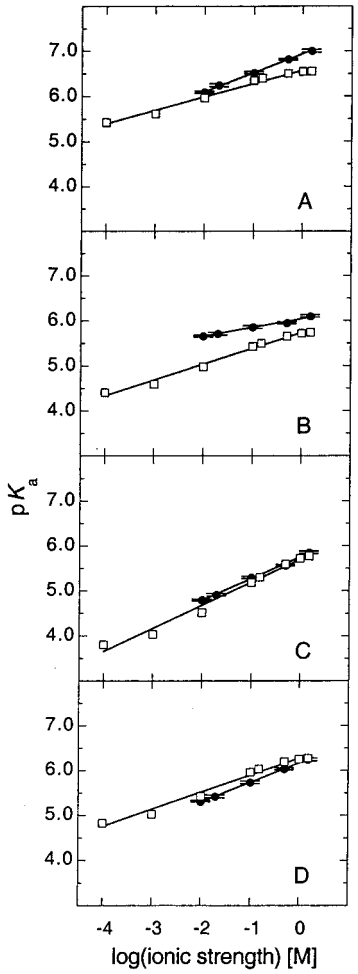

FIGURE 3: Comparison of measured (solid circles) and calculated (open squares) KCl dependence of pK_a values of His-8 (A), His-46 (B), His-121 (C), and His-124 (D). Straight lines are only meant to guide the eye.

The salt dependencies of experimental and calculated pK_a values are compared in Figure 3. The calculations reproduced the salt dependence of pK_a values measured in KCl rather well, even though the salt effects on solvation energies were not included in these calculations for reasons discussed previously (*12*). The ionic strength dependence of the solvation energy is responsible for a net ΔpK_a of 0.20 between 0.01 and 1.5 M (*12*). Explicit treatment of the ionic strength dependence of the solvation energy would have improved the agreement between calculations and experimental data in the case of His-46 and His-124, but it would have slightly worsened the agreement in the case of His-8 and His-121. The agreement between calculated and measured pK_a values in the presence of the SO_4^{2-} and SCN^- salts was less impressive. This is not surprising because not all of the effects of these two anions can be captured with the concept of ionic strength, which is the only parameter used to calculate the salt dependence of pK_a values with the linearized Poisson−Boltzmann equation. The significance of the agreement between calculated and observed KCl effects on pK_a values stems from the fact that KCl is relatively

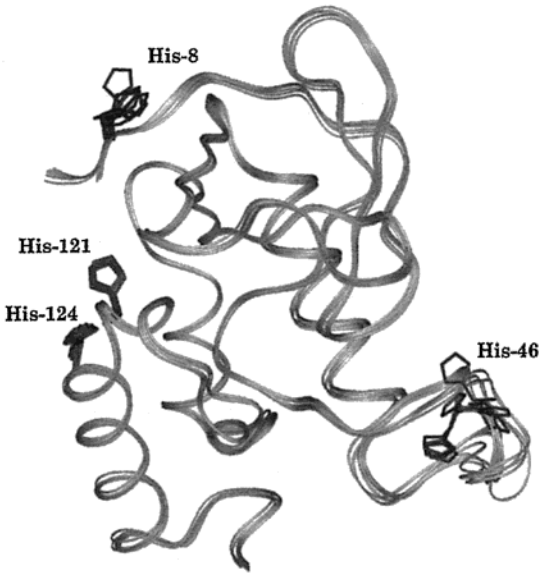

FIGURE 4: Superposition of the backbones of eight crystallographic structures of SNase (1stn, 1snc, 2snm, 1ey4, 1ey5, 1ey0, 1stg, and 1sth) with resolution ranging from 1.6 to 1.97 Å. Histidine side chains are shown. The structures were superimposed by overlapping the trace backbone of the 7−140 segment.

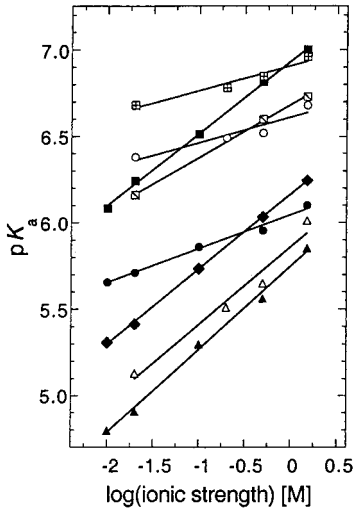

FIGURE 5: Comparison of the salt dependence of histidine pK_a values in SNase, myoglobin, and model peptides. Data included are His-8 (solid squares), His-46 (solid circles), His-121 (solid triangles), and His-124 (solid diamonds) in SNase; data for His-12 (open circles) and His-113 (open triangles) from sperm whale myoglobin; and GHG (crossed squares) and FKHLK (hatched squares) obtained previously (*12*). Lines are only meant to guide the eye.

neutral with respect to salt-specific effects and Hofmeister-related phenomena, and its effects can be described effectively in terms of the concept of ionic strength in the calculations (*35*).

The best agreement between the observed and the calculated behavior over the experimental range of KCl concentrations was for His-121 and His-124. In the case of His-8, the agreement was good at salt concentrations ≤0.10 M, and deteriorated at higher ionic strength as the calculated dependence was shallower than the measured effect. The region of the protein encompassing His-8 is dynamic, and the first five residues of SNase are missing from the crystallographic structure. This N-terminal segment includes the N-terminus and Lys-5, which could not be taken into account in the calculations, and whose presence should steepen the predicted salt dependence. Thus, the discrepancy between calculated and observed values for His-8 might reflect the absence of these residues in the crystallographic structure used in the calculations.

The greatest discrepancy between calculated and measured pK_a values was for His-46, especially at low salt concentrations. The calculated salt sensitivity of His-46 was steeper than observed experimentally. These problems with the estimation of the pK_a values of His-46 with a static structure were expected. The structures in Figure 4 show that His-46 is located in a flexible loop that can exist in a large number of conformations in both NMR (*40*) and crystallographic structures (*34, 41*). The calculations were performed on a single, static structure, and apparently in the case of His-46, the crystallographic structure does not reflect the average of the configuration ensemble populated in solution. The agreement between calculated and experimental pK_a values of His-46 could probably be improved, by averaging pK_a values calculated in different conformers, or by exploring conformational flexibility explicitly in this region of the protein with molecular dynamics simulations (*14, 42*−*44*).

DISCUSSION

Comparison of Salt Sensitivity of Histidine pK_a Values in Model Compounds, in Myoglobin, and in SNase. The ionization of histidines in model compounds and in sperm whale and horse heart myoglobin was found previously to be moderately sensitive to NaCl in the range 0.02−1.5 M (*12*). In this range of salt concentration, the average increase in the pK_a values of most histidines in myoglobin is 0.4 unit. The notable exceptions are the following: His-36, which is presumably ion-paired to Glu-38 and has a pK_a that is insensitive to salt; His-48, which is insensitive to salt for reasons that are not well understood; and His-113, which is in van der Waals contact with the guanidinium moiety of Arg-31 and has a steep dependence on salt concentration. The pK_a value of the histidine in the FKHLK peptide is also dependent on salt concentration, presumably because interactions between the imidazolium and the net +2 charge are screened at high salt concentration. In comparison to the general trends observed in myoglobin and in model compounds, the pK_a values of histidines in SNase are highly salt sensitive.

Figure 5 highlights differences in the salt sensitivity of histidines in SNase, in myoglobin, and in model compounds. Included in this figure are pK_a values of the four histidines in SNase, of two histidines representing the most common behavior among the cases studied previously (His-12 in myoglobin and the histidine in the GHG peptide), and of two histidines representing those with the steepest salt dependence among the cases studied previously (His-113 in myoglobin and the histidine in the FKHLK peptide). Two differences are immediately obvious. First, over the entire range of salt concentrations studied, the pK_a values of histidines 46, -121, and -124 of SNase are depressed relative to model compound values. Only His-8 titrates with a normal pK_a value. Second, the salt dependencies of His-8, His-121, and His-124 are 2−3 times greater than the response

observed in most histidines in myoglobin and in model compounds. When the salt concentration is raised from no added salt to 1.5 M KCl, these three histidines exhibit shifts of approximately 1 full pK_a unit. This is similar to the response of His-113 in myoglobin, and more pronounced than that of the histidines in the FKHLK peptide (*12*). It is noteworthy that His-8, which titrates with a pK_a in the normal range at all salt concentrations studied, exhibits a salt sensitivity comparable to that of histidines found in basic environments or with depressed pK_a values. His-46, which also has a depressed pK_a value, exhibits a milder salt sensitivity than the other histidines in SNase, but still greater than the average sensitivity in myoglobin.

The effects of salts on pK_a values of the majority of histidines in myoglobin and in peptides were interpreted previously in terms of the preferential stabilization of the charged form of histidine with increasing salt concentrations due to interactions between histidinium and counteranions (*12*). This interpretation was suggested by the similar behavior of histidine residues in myoglobin and in neutral peptides such as cGH, pEHGa, in imidazole, and in the charged but neutral GHG. It was supported by calculations of the effects of salt on solvation energies of imidazole with Poisson−Boltzmann continuum electrostatics methods. The experimental data suggest that the details of the protein environment have minimal influence on the salt sensitivity of most histidines in myoglobin. They also suggest that screening of electrostatic interactions among surface charges does not contribute significantly to the salt dependence of pK_a values. This means that net contributions to the pK_a values by Coulombic interactions among surface charged groups are negligible, either because interactions are weak or because repulsive and attractive interactions are balanced and cancel each other.

The calculated salt dependence of the solvation energy of histidines will always predict an increase in the pK_a value with increasing salt concentration. This effect must contribute to the observed increase in the pK_a values of histidines in SNase at high salt concentration; however, the salt dependence of the solvation energy can only account for pK_a shifts of 0.2−0.3 unit (*12*). Other factors must be primarily responsible for the steep salt dependence of histidine pK_a values in SNase. Note that in Figure 5, the slope of the salt dependence of pK_a values of His-8, His-121, and His-124 in SNase is similar to that of His-113 in myoglobin, whose pK_a increases by 0.9 unit between 0.02 and 1.5 M NaCl. This pK_a shift is in the direction expected if an unfavorable electrostatic interaction were progressively screened by increasing concentrations of counterions, consistent with the 3.8 Å average distance between Nϵ1 and Nδ2 of His-113 and the Nη atoms of Arg-31 in sperm whale myoglobin. All contacts shorter than 5.8 Å between the four histidines in SNase and polar and charged atoms are listed in Table 2. Surprisingly, in the case of SNase, there are no positively charged atoms within 6 Å of any of the histidines except for the Nζ of Lys-49, which is 5.8 Å from His-46 (*34, 41*). Conformational fluctuations of the lysine side chains could position positive charges closer to the histidines than is reflected in the static, crystallographic structures, but it remains unlikely that short-range electrostatic interactions are directly responsible for the depressed pK_a values of basic residues in SNase, or for their salt sensitivity.

Table 2: Polar and Ionic Contacts of Imidazole Nitrogen Atoms of Histidines in SNase[a]

atom *i*	SA_i[b]	r_{ij} (Å)[c]	atom *j*	residue *j*
His-8 ND1	0.61	4.17	N	Lys-9
		4.28	OE2	Glu-10
		4.35	O	Lys-9
		5.19	OE1	Glu-10
		5.26	N	Glu-10
His-8 NE2	0.60	4.10	OE2	Glu-10
		5.22	NH1	Arg-81
		5.43	OE1	Glu-10
		5.58	O	Lys-6
		5.59	N	Lys-9
His-46 ND1	0.01	2.72	N	Lys-49
		2.95	N	Lys-48
		3.29	N	Pro-47
		3.97	N	Gly-50
		4.88	O	Lys-48
		5.06	O	Pro-47
		5.10	OE2	Glu-52
		5.23	O	Gly-50
		5.38	OE1	Glu-52
		5.39	O	Lys-49
His-46 NE2	0.73	4.34	N	Pro-47
		4.39	N	Lys-48
		4.62	N	Lys-49
		4.66	OE2	Glu-52
		4.66	OE2	Glu-43
		5.07	OE1	Glu-52
His-121 ND1	0.34	4.02	O	Thr-120
		5.16	OE1	Glu-75
		5.26	OH	Tyr-93
		5.37	OH	Tyr-91
		5.43	N	Glu-122
His-121 NE2	0.01	3.06	OE1	Glu-75
		3.71	OH	Tyr-93
		4.42	OE2	Glu-75
		5.13	OH	Tyr-91
		5.33	SD	Met-98
		5.53	O	Thr-120
His-124 ND1	0.84	4.68	N	Leu-125
		5.12	OG	Ser-128
His-124 NE2	0.50	4.84	OE2	Glu-101
		4.92	OE1	Glu-101
		5.11	OG	Ser-128
		5.26	N	Leu-125

[a] Only contacts shorter than 5.8 Å are included. [b] SA_i represents the water-accessible surface area, normalized using the water accessibility in Gly-X-Gly peptides (*21*). Fully water-accessible groups have $SA_i = 1$, and those that are fully buried have $SA_i = 0$. [c] Distances calculated with the 1stn structure of Hynes and Fox (*34*).

Molecular Origins of Depressed pK_a Values. Two factors could explain the depressed pK_a values of histidines in SNase relative to model compounds: (1) repulsive electrostatic interactions with other surface basic groups, and (2) dehydration upon removal from bulk solvent. The similarity in the salt sensitivity measured experimentally for His-121 and His-8 despite their different pK_a values argues that non-Coulombic effects are responsible for the baseline pK_a values at low salt concentration. This was established by dissection of calculated pK_a values into energetic contributions from Coulombic interactions and from self-energies. In the computational model that was used to calculate pK_a values, the self-energy term contains contributions from interactions between the ionizable group and permanent dipoles in the protein, and from the Born term to capture the reaction field energy (*42*). The Born term accounts for the difference in the self-energy related to differences in the polarizability of water and of the protein interior. The data in Table 3 reveal

Table 3: Energetic Contributions to Calculated pK_a Values at 25 °C

	His-8		His-46		His-121		His-124	
	1mM	1.5 M	1mM	1.5 M	1mM	1.5 M	1mM	1.5 M
p$K_{1/2}$[a]	5.61	6.55	4.60	5.75	4.03	5.78	5.02	6.27
ΔpK_a[b]	−0.69	0.25	−1.70	−0.56	−2.27	−0.52	−1.28	−0.03
ΔG_{ij}[c,d]	0.36	−0.86	0.56	−0.76	1.51	−0.68	0.60	−0.95
ΔG_{ii}[c,e]	0.57	0.53	1.76	1.52	1.57	1.40	1.14	0.99
ΔG_{Born}[c,f]	0.46	0.47	0.55	0.54	0.78	0.78	0.75	0.75
ΔG_{bkgd}[c,g]	0.11	0.06	1.21	0.97	0.79	0.62	0.38	0.25

[a] pH at the point where the site is half-charged. [b] Calculated shift in pK_a relative to the model compound value of 6.3. [c] All ΔG in kcal/mol. [d] This term represents the sum of all pairwise, Coulombic interactions. It was calculated as $|1.36*\Delta pK_a| - \Delta G_{ii}$. It could have also been calculated by actually summing the contributions by all individual pairwise Coulombic interactions (ΔG_{ij}) at a pH where the group of interest is fully charged. The differences between the terms calculated in this way are negligible. [e] Self-energy, calculated as the sum of ΔG_{Born} and ΔG_{bkgd}. [f] Reaction field energy. This term reflects differences in the self-energy of an ionizable group in water and in the protein, arising from differences in the polarizabilities of these two environments. [g] Energy of interaction with permanent dipoles. "bkgd" signifies background.

that both the Coulombic and the self-energy terms contribute to the depressed pK_a values of histidines in SNase. Unfavorable self-energies imply that interactions with the local environment in the protein are not sufficient to compensate for the loss of solvation relative to a histidine in water. Even in very low ionic strength (1 mM), where Coulombic interactions are strongest, destabilizing contributions from the self-energy were greater than those from Coulombic interactions. In the case of His-121, which exhibits the most depressed pK_a value, the destabilizing contributions of repulsive interactions between histidines and other basic groups on the surface of SNase were comparable to the destabilizing contribution by the self-energy. Note that although the net consequence of Coulombic interactions in 1 mM ionic strength was to depress the pK_a values, at 1.5 M ionic strength the net contributions by Coulombic interactions were actually stabilizing. The reason that the pK_a values of His-46, His-121, and His-124 remained depressed at 1.5 M ionic strength is that under these conditions the self-energy is still unfavorable. The self-energy of His-8 is not as unfavorable as in the case of the other three histidines; thus, it titrates with a seemingly normal pK_a value. However, its interactions with other ionizable residues are similar to those of His-121 and His-124; thus, it exhibits the same strong salt sensitivity observed for the other three histidines.

Molecular Origins of the Salt Sensitivity of Histidine pK_a Values. The salt dependence of contributions by Coulombic, Born, and background energies presented in Figure 6 supports the idea that the striking salt dependence of the pK_a values reflects primarily the attenuation of Coulombic interactions by the ionic strength. The Born term and the background term are insensitive to salt throughout the studied range. Even in the case of His-46, which has the most salt-sensitive background term, the salt sensitivity of the Coulombic contributions to the pK_a is an order of magnitude greater (Table 3). In contrast, the calculated salt sensitivity of Coulombic interactions was dramatic for all four histidines, and it paralleled closely the net effects of salt on pK_a values.

The Coulombic contributions to the pK_a values were dissected further into contributions by attractive and repulsive interactions with other charged groups closer or further than

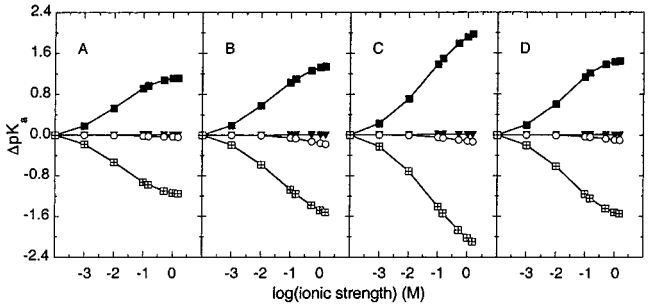

FIGURE 6: Decomposition of the salt dependence of pK_a values calculated by continuum methods (solid squares) into contributions by Coulombic (crossed squares), Born (solid inverted triangles), and background (open circles) energies. Data for His-8 (A), His-46 (B), His-121 (C), and His-124 (D) are shown. All curves have been normalized to reflect the shifts in pK_a values with increasing ionic strength relative to each group's computed pK_a values in the absence of salt [i.e., ΔpK_a = pK_a(ionic strength) − pK_a(0 M)]. Absolute values of these energies are described in Table 2.

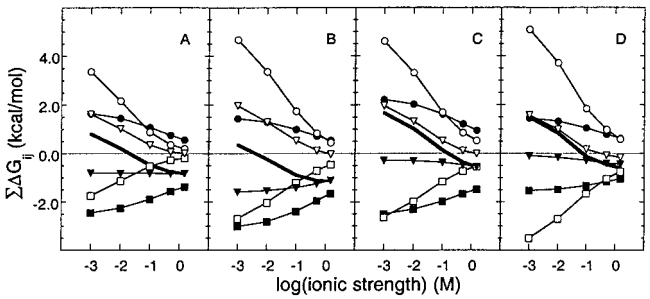

FIGURE 7: Salt dependence of Coulombic interactions of His-8 (A), His-46 (B), His-121 (C), and His-124 (D), calculated with the continuum method. The sum of all Coulombic interactions (thick line) was dissected into contributions from attractive (open squares) and repulsive (open circles) long-range interactions with $r_{ij} > 10$ Å, and into attractive (solid squares) and repulsive (solid circles) medium- and short-range interactions with $r_{ij} \leq 10$ Å. Also shown are the sum of all long-range interactions with $r_{ij} > 10$ Å (open triangles), and the sum of all medium- and short-range interactions with $r_{ij} \leq 10$ Å (closed triangles).

10 Å. The salt dependence of these different contributions is shown in Figure 7. According to these data, both medium-range ($r_{ij} \leq 10$) and long-range ($r_{ij} > 10$) Coulombic interactions contributed significantly to the pK_a values of the four histidines, although in fact the contributions by medium-range interactions are weak in the cases of His-121 and His-124. Long-range repulsive interactions were stronger than either long-range attractive, medium-range attractive, or medium-range repulsive interactions. The sum of all medium-range interactions was stabilizing for all histidines, but the sum of long-range interactions was destabilizing. At low ionic strengths, the net contributions by long-range repulsive interactions are dominant. However, they decrease steeply with increasing ionic strength, more steeply than medium-range ones, and they weaken considerably in 1.5 M KCl. Note in this figure that while all histidines experience net repulsive interactions at low ionic strength, they all sense net favorable electrostatic potentials at higher ionic strength.

The calculated values in Figure 7 suggest that the salt sensitivity of pK_a values in SNase arises from the screening of long-range Coulombic interactions. For comparison, note that the screening of the +2 charge in the FKHLK peptide between 0.02 and 1.5 M NaCl yields a ΔpK_a of 0.6, which is approximately only half the shift observed for these three

histidines in SNase. The more dramatic case of the histidines in SNase must reflect the greater abundance of arginines and lysines on the surface of the protein, which in aggregate produce substantial destabilizing electrostatic fields susceptible to screening by counterions. One of the most important implications of these experimental studies is that, at least in the case of highly charged proteins with isoionic points far from neutral pH, such as SNase, weak pairwise electrostatic interactions between charges separated by more than 10 Å can add to yield substantial effects.

The sensitivity of His-46 to KCl concentration deserves special mention. It is shallower and more similar to that of the histidine in the FKHLK peptide, which more closely emulates the context of His-46 in the primary sequence. The crystallographic structures in Figure 4 show that His-46 resides on a loop that projects away from the main globular portion of the protein, and which can exist in many conformations. In some crystallographic structures, this loop is not even visible. The lower sensitivity of His-46 to salt concentration suggests that its interactions with other charges are weaker than those of the other histidines. This probably reflects the dynamic character of this segment of the protein. The experimental data suggest that His-46 still senses the substantial positive charge in residues 43−53 forming the flexible loop, or in the rest of the protein; thus, its pK_a remains markedly salt-sensitive.

Charge Distribution around Histidines. It is interesting to note that the calculated salt sensitivities of His-8, His-121, and His-124 are very similar despite the differences in their pK_a values. This would appear to contradict Linderstrøm-Lang's notion that the salt sensitivity of pK_a values is related to their distance to the isoionic point of the protein. Specifically, the distance of the pK_a value of His-8 to the isoionic point of the protein is shorter than that of the other histidines, yet His-8 exhibits a salt sensitivity similar to those of His-121 and His-124. Similarly, the pK_a value of His-46 is halfway between the pK_a values of His-121 and His-8, yet it exhibits a shallower salt dependence. However, the net charge of SNase in the pH range 5−7 changes by only 5 units (*4*). This does not constitute a sufficiently large change in net charge to test Linderstrøm-Lang's hypothesis, especially when medium- and long-range interactions are weak.

One reason that His-8, His-121, and His-124 have similar salt sensitivity is that the combined effects of electrostatic interactions over the full range of intercharge distances are equivalent in these three cases. This is illustrated in Figure 8, which shows the patterns of charge distribution around the four histidines in SNase and around four representative histidines in sperm whale myoglobin. These diagrams demonstrate that within a 30 Å radius of each of the histidines in myoglobin that exhibit salt-insensitive ionization behavior, such as His-12, His-81, and His-116, each negative charge is balanced by a positive charge found somewhere in the protein at a similar distance. Hence, within this radius, electrostatic interactions between the histidine and other ionizable groups cancel. This distribution of repulsive and attractive interactions is consistent with the similarity in the salt sensitivity of these histidines and of histidines in neutral peptides. It shows that the reason that the salt sensitivity of these histidines parallels that of the self-energy, rather than that of the Coulombic interactions, is not that Coulombic

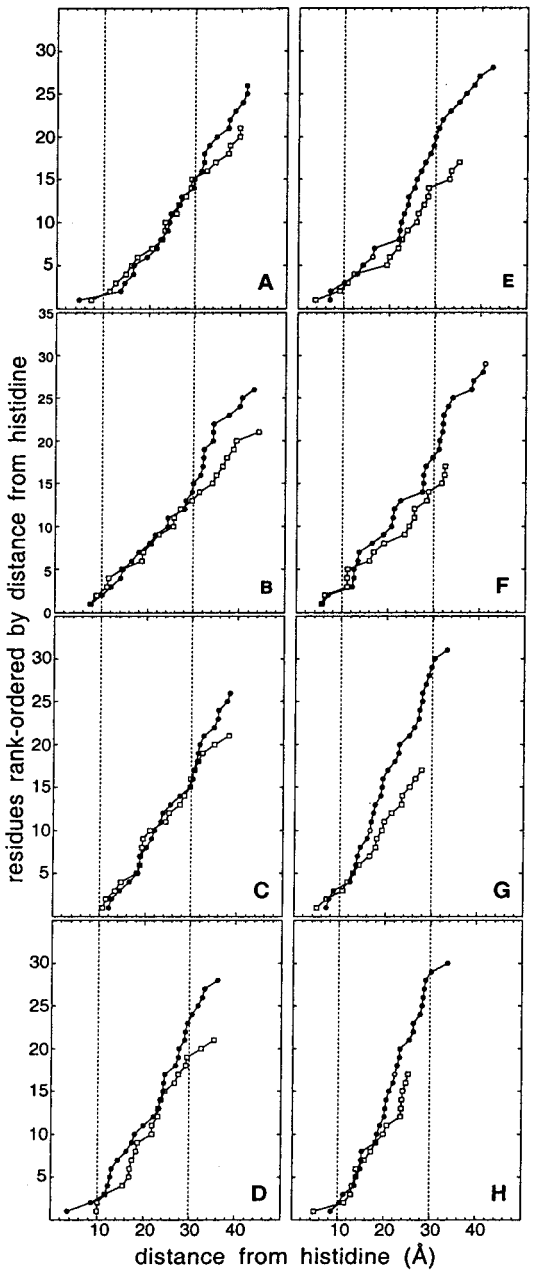

FIGURE 8: Rank-ordered distances between histidines and basic (solid circles) and acidic (open squares) residues in myoglobin (A−D) and SNase (E−H): (A) His-12, (B) His-81, (C) His-116, (D) His-113, (E) His-8, (F) His-46, (G) His-121, and (H) His-124. Distances were calculated between the Cϵ atom in histidines and the Nζ, Cζ, Cϵ, Cδ, and Cγ atoms in Lys, Arg, His, Asp, and Glu, respectively, using the 4mbn myoglobin structure (*48*) and the 1stn nuclease structure (*34*). The dotted vertical lines at r_{ij} = 10 and 30 Å are meant to highlight the regime of charge−charge interactions that determine the steep salt sensitivity of histidines in SNase.

interactions are insensitive to salt. Because attractive and repulsive interactions are well balanced, the net salt effect on Coulombic interactions is null. In contrast, the distribution of acidic and basic residues around His-113 in myoglobin is not balanced. In addition to its direct contact with Arg-31, there are several other basic residues in the 10−15 Å radius that are not balanced by acidic groups at similar distances. Hence, the local environment around His-113 is expected to be electropositive, and subject to screening by counterions, which renders its pK_a value highly salt-sensitive.

The three histidines in SNase that exhibited sensitivity to salt comparable to that of His-113 also have unbalanced distribution of charges around them. His-8, His-121, and His-124 do not make direct contact with a basic group as in the case of His-113; the charge within a 10 Å radius around these histidines is evenly distributed. This can be seen in the overlapping plots of the rank-ordered distribution of distances to acidic and basic residues (Figure 4E−H). However, beyond 10 Å, the curves for acidic and basic residues diverge from each other; the radial charge density for positively charged groups is greater than for acidic groups beyond this radius. For His-124, charge imbalance begins at a radius of 20 Å. Charge imbalance around each of the four histidines in SNase is evident within a 10−25 Å radius. This suggests that the cumulative effects of specific imbalances in charge distribution at medium- and long-range, rather than net protein charge or short-range interactions, is the primary determinant of the salt sensitivity of the histidines in SNase.

The experimental pK_a values were reproduced better by the continuum calculations in SNase than in myoglobin and in other proteins (*11*, *12*, *45*). In myoglobin and other proteins, the magnitudes of electrostatic interactions are exaggerated for reasons that are not entirely obvious. One possibility is that the calculations fail in cases or under conditions where dynamics and conformational fluctuations are significant, such that the static crystallographic structures used in the calculations misrepresent the distribution of distances between charged atoms in solution. Explicit treatment of dynamics might improve the agreement between calculated and experimental pK_a values, as might the ad hoc use of even higher effective dielectric constants to attenuate the energy of pairwise interactions. This was corroborated by the observation that the modified Tanford−Kirkwood algorithm, which employs effective dielectric constants >42, captures the absolute magnitude of pK_a values of histidines in myoglobin in 0.10 M ionic strength better than the more rigorous calculations based on finite difference solution of the linearized Poisson−Boltzmann equation (*12*).

Specific Salt Effects. The calculated salt dependence of pK_a values is determined exclusively by the ionic strength term in the Poisson−Boltzmann equation. The good agreement between the calculated and measured salt dependence of pK_a values suggests that the salt effects were dominated by the screening of Coulombic interactions proportional to the ionic strength. The effects of K_2SO_4 and KSCN on pK_a values were measured to test this. These salts were selected because SO_4^{2-} and SCN^- lie at opposite extremes of the Hofmeister series for anions, and Cl^- is a Hofmeister-neutral anion (*35*). The slopes of the pK_a vs ionic strength graphs for these three salts are consistent with what is expected from their rank order in the Hofmeister series: the slope of the salt dependence is steepest for SCN^-, intermediate for Cl^-, and shallowest for SO_4^{2-} (Figure 2). The data clearly demonstrate that in addition to the ionic strength effect proper, there is a component of the observed salt effect that is related to direct interactions between protein and anions. Although it is difficult to describe in greater detail the molecular origins of the anion-specific effects, particularly the anion-specific dependence of absolute pK_a values, it is interesting to speculate about likely origins of these effects.

The greater effect of SCN^- on pK_a values of histidines in SNase compared to the histidines in the neutral cGH and pEHGa peptides suggests that the protein environment enhances the effects specific to SCN^-. This might be related to the high density of basic groups in SNase, or to binding of SCN^- to polar groups (*35*). SCN^- can establish multivalent contacts with proteins; its greater influence on pK_a values might simply reflect more effective binding interactions than Cl^- (*37*). Similarly, SO_4^{2-} is a large anion, known to interact specifically with proteins through electrostatic and hydrogen bonding interactions. The ability of SO_4^{2-} to interact with proteins is also consistent with the higher histidine pK_a values at low concentrations of SO_4^{2-}, and with the lack of convergence in the limit of low ionic strength with the values measured in SCN^- and Cl^-. SO_4^{2-} might even exert its influence through a polyelectrolyte effect similar to that observed in highly acidic biopolymers.

The characteristic response of the different histidines to the different types of anions might also be related to the inherent flexibility of their microenvironments. Differences among the effects of Cl^-, SO_4^{2-}, and SCN^- are largest for His-121 and His-124. These two histidines are both found in the structurally constrained crevice between the third α-helix and the β-sheet portion of the protein. The position of the side chain of each of these histidines is invariant among many crystallographic and NMR structures (Figure 4). The enhanced effect of SCN^- observed for both His-121 and His-124 might be related to the accumulation of anions in this rigid region in excess of what is predicted by Poisson−Boltzmann electrostatics, through the mechanisms described above. In fact, even the adsorption of SCN^- to apolar surfaces may contribute to its significant effects on pK_a values. Anions with low charge density such as SCN^- are readily excluded from bulk solvent; thus, they could be concentrated locally owing to the partially apolar composition of the protein surface in the neighborhood of these histidines. The increased local counterion concentration would result in a greater effect than might be expected from ionic strength considerations alone (*35*). Similarly, the effects of SO_4^{2-} are also most different from the effects of Cl^- for the cases of His-121 and His-124. This may reflect the specific association of the SO_4^{2-} anion with histidinium groups, as suggested by the NMR-monitored protonation curves for His-121 and His-124. The titration curves of these histidines in the presence of SO_4^{2-} are not only shifted to higher pK_a values but are also noticeably steeper than the curves in the presence of Cl^- (data not shown). The ionization of His-121 and His-124 might be coupled to SO_4^{2-} binding to the shallow pocket between these two residues.

In contrast, the ionization curves of His-8 and His-46 in the presence of Cl^- and SO_4^{2-} are of similar shape and steepness. Apparently neither one of these sites offers as favorable an environment for SO_4^{2-} association as His-121 or His-124. In fact, His-8 and His-46 do not discriminate effectively among the different anions, and this might be related to their unstructured environments. The loose conformation of the backbone around His-46 was discussed previously. Three factors suggest that His-8 in solution is also not fixed in a unique, singularly constrained position. (i) As shown in Figure 4, the position of His-8 shows some variability among different various crystallographic structures. (ii) Temperature factors for this residue are high,

suggesting it is either relatively unstructured or exists in multiple conformations within a single protein crystal. (iii) Portions of the peptide chain preceding His-8 in sequence are not resolved crystallographically, suggesting that this N-terminal stretch of SNase is fairly flexible, or at least subject to conformational heterogeneity. In light of this, it is reasonable to expect that both His-8 and His-46 will be better solvated and less prone to ion-specific influences than the other two histidines. His-8 is closer to the globular core than His-46, which may explain its greater sensitivity to salt conditions despite its inferred flexibility. The strong dependence on SCN^- compared to Cl^- indicates that anionic adsorption of strongly chaotropic anions may occur near His-46.

Relationship between Salt Effects on Histidine pK_a Values and Global Stability of SNase. The pK_a values of histidines and their steep salt dependence have interesting implications about the molecular basis of the salt- and proton-linked stability of SNase. The shifts in the pK_a values of the four histidines between 0.01 and 1.5 M salt add up to 3.34 pK_a units, equivalent to 4.5 kcal/mol at 25 °C. The change in global stability between 0.10 and 1.0 M salt predicted from the salt dependence of histidine pK_a values is 2.0 kcal/mol. Only half of the predicted increase in stability is observed in the free energy difference between the native and denatured states measured by urea denaturation (*4*). The depressed pK_a values of the histidines in the native state should also give rise to a substantial pH dependence of the stability in the pH range where they titrate. The difference between the pK_a values of the histidines in the native state in 0.10 M salt, and the pK_a of 6.6 of histidine in model compounds at the same salt concentration, is energetically equivalent to 4 kcal/mol. This is consistent with the pH dependence of stability obtained by numerical integration of potentiometric proton binding curves measured in native and denaturing conditions. However, the stability measured by temperature and urea denaturation does not exhibit the expected pH dependence (*4*). Similarly, mutants of SNase with global stability of approximately 3 kcal/mol or less should undergo acid denaturation in the range of pH where histidines titrate. This is also not observed experimentally (*46*). These contradictory observations suggest either that the histidines titrate with nativelike pK_a values in the denatured state (*4*) or that the stability measured by the linear extrapolation method assuming a two-state model is not valid in the case of SNase (*47*), or both. The difficulty in reconciling the properties of histidines observed by ^{1}H NMR spectroscopy in the native state of SNase, with other thermodynamic measurements, suggests that there are issues related to the electrostatic contributions to the folding and stability of SNase that remain to be explained.

Conclusions. The marked salt sensitivity of the pK_a values of histidines in SNase reflects an imbalance in the distribution of acidic and basic residues around the histidines. Charge imbalance is inherent in proteins with asymmetric charge distribution, but even proteins that have an equal number of acidic and basic residues distributed symmetrically on the surface can exhibit charge imbalance at pH values far from their isoionic point. As demonstrated in this study, in highly charged proteins where charge imbalance exists, weak medium- and long-range electrostatic interactions can cumulatively give rise to highly salt-sensitive electrostatic effects.

Structure-based calculations with a static structure and a continuum model based on the linearized Poisson−Boltzmann equation reproduced the Cl^-dependence of pK_a values, but only when the protein interior was treated empirically with $\epsilon_{in} = 20$. The agreement between calculated and experimental behavior suggests that some properties of the ionic double layer around proteins were described quantitatively by the mean-field approximation inherent in Poisson−Boltzmann electrostatics. According to the calculations, the pK_a values are depressed because of unfavorable self-energies and repulsive Coulombic interactions, and the unusual salt sensitivity of the histidines in SNase is determined mainly by screening of repulsive, Coulombic interactions with charges more than 10 Å away. To test further the ability of these computational methods to reproduce accurately the magnitude of surface electrostatic effects in proteins, it will be necessary to measure the energy of pairwise charge−charge Coulombic interactions experimentally.

ACKNOWLEDGMENT

We gratefully acknowledge Dr. Charles Long for expert technical advice with the Varian 500 MHz NMR, and Prof. Kim Collins for insightful comments and criticism.

REFERENCES

1. Oliveberg, M., Vuilleumier, S., and Fersht, A. (1994) *Biochemistry 33*, 8826−8832.
2. Oliveberg, M., Arcus, V. L., and Fersht, A. R. (1995) *Biochemistry 34*, 9424−9433.
3. Tan, Y. J., Oliveberg, M., Davis, B., and Fersht, A. R. (1995) *J. Mol. Biol. 254*, 980−992.
4. Whitten, S. T., and García-Moreno E., B. (2000) *Biochemistry 39*, 14292−14304.
5. Kuhlman, B., Luisi, D., Young, P., and Raleigh, D. (1999) *Biochemistry 38*, 4896−4903.
6. Swint-Kruse, L., and Robertson, A. D. (1995) *Biochemistry 34*, 4724−4732.
7. Stites, W. E., Gittis, A. G., Lattman, E. E., and Shortle, D. (1991) *J. Mol. Biol. 221*, 7−14.
8. García-Moreno E., B., Dwyer, J., Gittis, A., Lattman, E., Spencer, D., and Stites, W. (1997) *Biophys. Chem. 64*, 211−224.
9. Dwyer, J., Gittis, A., Karp, D., Lattman, E., Spencer, D., Stites, W., and García-Moreno E., B. (2000) *Biophys. J. 79*, 1610−1620.
10. Dao-pin, S., Anderson, D. E., Baase, W. A., Dahlquist, F. W., and Matthews, B. W. (1991) *Biochemistry 30*, 11521−11529.
11. Forsyth, W. R., Gilson, M. K., Antosiewicz, J., Jaren, O. R., and Robertson, A. D. (1998) *Biochemistry 37*, 8643−8652.
12. Kao, Y.-H., Fitch, C. A., Bhattacharya, S., Sarkisian, C. J., Lecomte, J. T. J., and García-Moreno E., B. (2000) *Biophys. J. 79*, 1637−1654.
13. Antosiewicz, J., McCammon, A. J., and Gilson, M. K. (1996) *Biochemistry 35*, 7819−7833.
14. Antosiewicz, J., McCammon, J. A., and Gilson, M. K. (1994) *J. Mol. Biol. 238*, 415−436.
15. Pace, C., Alston, R., and Shaw, K. (2000) *Protein Sci. 9*, 1395−1398.
16. Shaw, K. L., Grimsley, G. R., Yakovlev, G. I., Makarov, A. A., and Pace, C. N. (2001) *Protein Sci. 10*, 1206−1215.
17. Loladze, V., Ibarra-Molero, B., Sanchez-Ruiz, J., and Makhatadze, G. (1999) *Biochemistry 38*, 16419−16423.
18. Spector, S., Wang, M., Carp, S., Robblee, J., Hendsch, Z., Fairman, R., Tidor, B., and Raleigh, D. (2000) *Biochemistry 39*, 872−879.

19. Sanchez-Ruiz, J. M., and Makhatadze, G. I. (2001) *Trends Biotechnol. 19*, 132−135.
20. Linderstrøm-Lang, K. (1924) *Compt. Rend. Trav. Lab. Carlsberg 15*, 7.
21. Matthew, J. B., Gurd, F. R. N., García-Moreno E., B., Flanagan, M. A., March, K. L., and Shire, S. J. (1985) *CRC Crit. Rev. Biochem. 18*, 91−197.
22. Shortle, D., and Meeker, A. (1986) *Proteins: Struct., Funct., Genet. 1*, 81−89.
23. Fuchs, S., Cuatrecasas, P., and Anfinsen, C. (1967) *J. Biol. Chem. 242*, 4768−4770.
24. Lecomte, J. T. J., and Cocco, M. J. (1990) *Biochemistry 29*, 11057−11067.
25. Cocco, M. J., Kao, Y. H., Phillips, A. T., and Lecomte, J. T. J. (1992) *Biochemistry 31*, 6481−6491.
26. Bhattacharya, S., and Lecomte, J. T. J. (1997) *Biophys. J. 73*, 3241−3256.
27. Wishart, D. S., Bigam, C. G., Yao, J., Abildgaard, F., Dyson, H. J., Oldfield, E., Markley, J. L., and Sykes, B. D. (1995) *J. Biomol. NMR 6*, 135−140.
28. Glasoe, P. K., and Long, F. A. (1960) *J. Phys. Chem. 64*, 188−190.
29. Li, N. C., Tang, P., and Mathur, R. (1961) *J. Phys. Chem. 65*, 1074.
30. Alexandrescu, A. T., Mills, D. A., Ulrich, E. L., Chinami, M., and Markley, J. L. (1988) *Biochemistry 27*, 2158−2165.
31. Markley, J. (1975) *Acc. Chem. Res. 8*, 70−80.
32. Davis, M. E., Madura, J. D., Luty, B. A., and McCammon, J. A. (1991) *Comput. Phys. Commun. 62*, 187−197.
33. Gilson, M. K. (1993) *Proteins: Struct., Funct., Genet. 15*, 266−282.
34. Hynes, T. T., and Fox, R. O. (1991) *Proteins: Struct., Funct., Genet. 10*, 92−105.
35. Collins, K. (1997) *Biophys. J. 72*, 65−74.
36. Goto, Y., Takahashi, N., and Fink, A. L. (1990) *Biochemistry 29*, 3480−3488.
37. Vaney, M. C., Broutin, I., Retailleau, P., Douangamath, A., Lafont, S., Hamiaux, C., Prange, T., Ducruix, A., and Ries-Kautt, M. (2001) *Acta Crystallogr., Sect. D: Biol. Crystallogr. 57*, 929−940.
38. Khare, D., Alexander, P., Antosiewicz, J., Bryan, P., Gilson, M., and Orban, J. (1997) *Biochemistry 36*, 3580−3589.
39. Sham, Y. Y., Muegge, I., and Warshel, A. (1998) *Biophys. J. 74*, 1744−1753.
40. Wang, J., Truckses, D. M., Abildgaard, F., Dzakula, Z., Zolnai, Z., and Markley, J. L. (1997) *J. Biomol. NMR 10*, 143−164.
41. Loll, P. J., and Lattman, E. E. (1989) *Proteins: Struct., Funct., Genet. 5*, 183−201.
42. Bashford, D., and Karplus, M. (1990) *Biochemistry 29*, 10219−10225.
43. Langsetmo, K., Fuchs, J. A., and Woodward, C. (1991) *Biochemistry 30*, 7603−7609.
44. You, T., and Bashford, D. (1995) *Biophys. J. 69*, 1721−1733.
45. Forsyth, W. R., and Robertson, A. D. (2000) *Biochemistry 39*, 8067−8072.
46. Whitten, S. T., Wooll, J. O., Razeghifard, R., García-Moreno E., B., and Hilser, V. J. (2001) *J. Mol. Biol. 309*, 1165−1175.
47. Baskakov, I. V., and Bolen, D. W. (1998) *Biochemistry 37*, 18010−18017.
48. Takano, T. (1977) *J. Mol. Biol. 110*, 569−584.

BI0119417